Surface Specific Heat of ^{3}He and Andreev Bound States

H. Choi, J. P. Davis, J. Pollanen, and W. P. Halperin

Department of Physics and Astronomy, Northwestern University, Evanston, Illinois 60208, USA

(Received 23 January 2006; published 31 March 2006)

High resolution measurements of the specific heat of liquid ^{3}He in the presence of a silver surface have been performed at temperatures near the superfluid transition in the pressure range of 1–29 bar. The surface contribution to the heat capacity is identified with Andreev bound states of ^{3}He quasiparticles that have a range of half a coherence length.

DOI: 10.1103/PhysRevLett.96.125301 PACS numbers: 67.57.Bc, 74.45.+c

Unconventional pairing superfluids and superconductors are sensitive to quasiparticle scattering at surfaces since all forms of scattering are inherently pair breaking [1]. Depending on the boundary conditions, whether scattering is specular or diffuse, and depending on the specific quantum state, the order parameter can be significantly suppressed. Correspondingly, quasiparticle bound states extend from a surface a distance approximately equal to the coherence length of the bulk superfluid. These states were first discussed by Andreev [2] in order to understand the difference between charge and thermal transport at superconducting interfaces, and they have been extensively investigated in unconventional superconductors. For example, the zero-bias conductance anomaly in tunneling experiments [3] has been ascribed to low-energy, surface bound states and provides a key indicator of unconventional pairing [4,5]. Andreev scattering [6] and Andreev bound states (ABS) are essential characteristics of thin superfluid films [7] of ^{3}He, and they dominate the properties of superfluid ^{3}He contained in the porous medium of silica aerogel [8,9]. In the latter case, the ABS lead to gapless superfluidity as has been determined from their influence on heat capacity [10] and thermal conductance [11]. The bound states affect physical measurements that use probes such as vibrating wires [12,13] for viscosity and thermometry experiments and crystal oscillators [14,15] for the measurement of the acoustic impedance.

Recently, Vorontsov and Sauls [7] have calculated the contribution to the free energy and specific heat of Andreev bound states in thin films of ^{3}He in the A phase. For a film on a solid surface having diffuse scattering boundary conditions, they find that there is a suppression of the superfluid transition T_c as well as a substantial reduction of the heat capacity in the superfluid state near T_c. Even for thick films, where the suppression effect on the transition temperature is negligible, the reduction of the heat capacity near the transition can be remarkably large. In this Letter, we present measurements of the contribution of these bound states to the heat capacity of superfluid ^{3}He near a silver surface close to the transition temperature.

Previous experimental work on ^{3}He in confined geometries has taken one of two approaches. The first is to investigate ^{3}He thin layers, for example, films with a free surface for studies of superfluid density [16], flow [17], and third sound [18] or in slabs having confinement on two sides, as was the case for a number of NMR experiments [19]. The other method is to determine the effects of surfaces on ^{3}He constrained in a porous medium, with the corresponding advantage of a larger effective surface area. If the pore structure is larger than the superfluid coherence length, the system can be approximated as a collection of randomly oriented planar surfaces. For measurements of the heat capacity, this latter approach is preferable. Earlier experiments [20–22] of this kind show that the heat capacity differs from that of the bulk, without a consensus for interpretation. Greywall suggested that there is a healing length of the superfluid at the surface [20]. Others have argued [21,22] that there is a broad distribution of transition temperatures of disconnected superfluid regions. In our experiment, we use a high resolution temperature sweep method that can provide sufficient detail to explore the temperature and pressure dependence of the heat capacity, and we keep some bulk ^{3}He present in the calorimeter as a reference. Near the transition, we observe a deficit in heat capacity with respect to the pure superfluid as was found in the thin film calculations of Vorontsov and Sauls. The model we develop is based on a surface specific heat from surface Andreev bound states. We find that the model can consistently account for our results as well as those from the earlier work.

Our measurements were performed with the calorimeter described by Choi *et al.* [10] for high resolution measurement of the specific heat of superfluid ^{3}He in silica aerogel. There are three regions of ^{3}He inside the calorimeter. The first is the interior of the silver heat exchanger constructed of sintered silver particles of micron size and has a volume $V_1 = 0.56 \pm 0.01$ cm^3 and surface area 2.9 ± 0.1 m^2. The second region is the open volume for bulk ^{3}He, $V_2 = 0.29 \pm 0.04$ cm^3. Finally, from our earlier studies [10], we have a disk of silica aerogel with pore volume of $V_3 = 1.06 \pm 0.01$ cm^3. The ^{3}He in the volume V_3 remains in the normal Fermi liquid state for all of the experiments reported here. We have previously determined its volume and heat capacity to an accuracy of 2%. We have subtracted

this contribution, plus the calorimeter background, from our measurements and do not discuss them further.

The samples were cooled by adiabatic demagnetization of $PrNi_5$, and the calorimeter was isolated from this refrigerator with a superconducting cadmium heat switch. The temperature of the sample cell was measured every 30 seconds using a SQUID based mutual inductance bridge for measurement of the magnetic susceptibility of a paramagnetic salt, La diluted CMN. Once the cadmium superconducting heat switch was open, the sample cell warmed at a rate $\dot{T}$ from an ambient heat leak $\dot{Q}$, typically 0.1 nW. Occasionally, we applied external heat pulses to check consistency and to calibrate this heat leak. Then the heat capacity was determined as

$$C = \frac{dQ}{dT} = \frac{dQ}{dt}\frac{dt}{dT} = \frac{\dot{Q}}{\dot{T}}. \quad (1)$$

The advantage of using slow-warming traces over the adiabatic heat pulse method is higher resolution. A heat pulse typically causes a temperature jump of 50–100 μK. In a slow warm-up trace, the temperature change for each point is less than 1 μK, and temperature disequilibrium within the ^{3}He and between ^{3}He and the thermometer is estimated to be less than 2 μK. However, such a small signal inherently results in poor signal to noise in determining $\dot{T}$. This can be overcome by averaging adjacent data points provided that the warm-up rate is adequately slow and stable. We used averaging to smooth the data, thereby decreasing our temperature resolution to 10 μK. All of our slow-warming data are reproduced by our pulsed heat capacity measurements, albeit with lower resolution in temperature.

On cooling through T_c, we observe a sharp, resolution-limited increase in the heat capacity, shown in Fig. 1, followed by a smooth increase and then a decrease over a range of temperature. For reference, we directly compare our results in this figure with the heat capacity measurements of bulk superfluid ^{3}He performed by Greywall [20]. The central question we address is what is the origin of the difference between these results. For bulk ^{3}He, we know that the jump in heat capacity at T_c, $\Delta C_s(T_c)$, corresponds to that of a BCS pairing system, enhanced by strong coupling [23]. The heat capacity then falls rapidly, approximately proportional to T^3. Consistently, in our data we find that there is a sharp increase in the heat capacity over a small range of temperature of 10 μK. It is natural to identify this jump with superfluid transition of the bulk ^{3}He in our calorimeter, and T_c is defined as the midpoint of this transition region. In Fig. 2, we show the difference between the measured heat capacity and that of the bulk superfluid for the same volume, $\delta C = C - C_s$ as a function of temperature at temperatures outside of the bulk ^{3}He transition region. The magnitude of the discontinuity in δC at T_c corresponds to the amount of ^{3}He in the silver heat exchanger given by the volume ratio $V_1/(V_1 + V_2) = \delta C(T_c)/\Delta C_s(T_c)$ and is plotted in Fig. 3. The apparent volume V_1, deduced in this way, is 0.40 ± 0.02 cm^3. As expected, it does not vary with pressure. The magnitude of the apparent volume is qualitatively consistent with an independent measurement, $V_1 = 0.56 \pm 0.01$ cm^3. Apart from experimental uncertainty, this discrepancy reflects difficulty in making an accurate extrapolation to T_c, which we discuss in greater detail below.

Below T_c, the behavior of the heat capacity must be attributed to the combination of the surface dominated heat

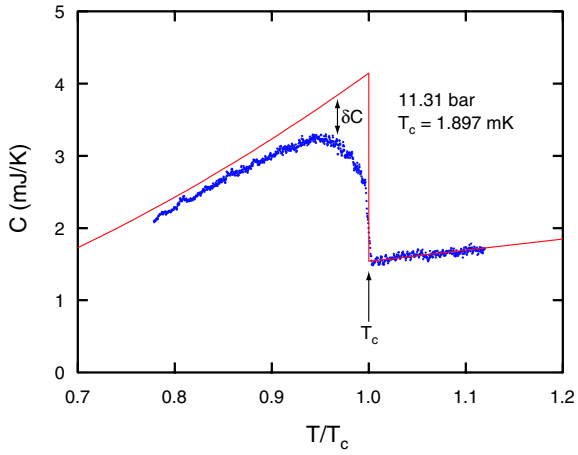

FIG. 1 (color online). Heat capacity of both bulk and confined ^{3}He obtained from a slow warm-up trace at 11.31 bar. The solid trace is the heat capacity expected for bulk ^{3}He determined from Greywall's measurements [20]. The data points are our measurements.

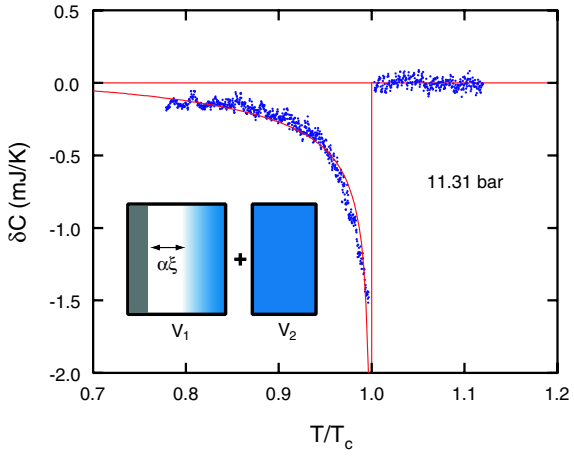

FIG. 2 (color online). $\delta C = (C - C_s)$ is the difference between the measured heat capacity C and that of the bulk superfluid C_s as a function of temperature at 11.31 bar. The inset is a sketch of the volume distribution in the calorimeter. V_1 is the fluid inside the silver heat exchanger and V_2 the volume outside. In our model, Andreev bound states reside within a distance $\alpha\xi(T, P)$ from the surface in the volume V_1; the rest of the ^{3}He in V_1 and all of that in V_2 is taken to be bulk superfluid. The model calculation, given by the smooth curve with a constant scale factor $\alpha = 0.48 \pm 0.08$, agrees well with the data.

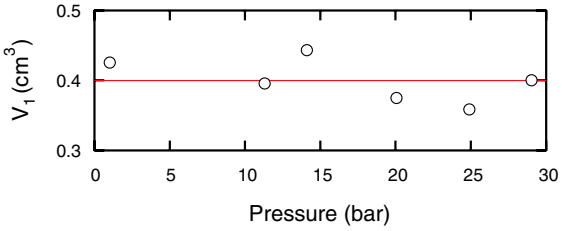

FIG. 3 (color online). Measurements of the heat capacity discontinuity at T_c interpreted as the volume in the heat exchanger, V_1 for various pressures.

capacity in the silver heat exchanger in addition to that of the bulk. The formation of surface bound states corresponds to transfer of spectral weight from above the energy gap to low energy (near the Fermi energy) with a density of states of low-energy excitations of order that in normal ^{3}He. Their spatial extent from the surface is expected [7,24] to be approximately that of the coherence length given by $\xi(T, P) = \xi_0(P)(1 - T/T_c)^{-1/2}$, where $\xi_0(P) = \hbar v_F/2\pi k_B T_c$. Here v_F is the Fermi velocity and k_B is the Boltzmann constant. On this basis, we propose a simple model where we take the surface heat capacity to be proportional to that of the normal fluid but constrained to a volume that scales as $A\xi(T, P)$, where A is the area of the silver surface. Consequently, we write the surface contribution to the heat capacity as $\alpha(T, P)\xi(T, P)Ac_n$, where c_n is the normal fluid specific heat. We investigate the temperature and pressure dependence of the scale factor α. A pictorial representation of this model is sketched in the inset in Fig. 2. The corresponding heat capacity is

$$C = \alpha(T,P)\xi(T,P)Ac_n + (V_1 + V_2 - \alpha(T,P)\xi(T,P)A)c_s$$
$$= (V_1 + V_2)c_s + \alpha(T,P)\xi(T)A(c_n - c_s) \quad (2)$$

and $\delta C = \alpha(T, P)\xi(T, P)A(c_n - c_s)$. Here c_s is the specific heat of bulk superfluid ^{3}He. The scale factor $\alpha(T, P)$ is the only unknown parameter necessary to describe the surface heat capacity and expresses the temperature dependence and pressure dependence of the surface heat capacity beyond that given by the coherence length and the normal specific heat.

We have used this model to interpret our measurements for various temperatures and pressures. For any given pressure, we find α is constant over the available range of temperature, down to $T/T_c \approx 0.7$. In Fig. 2, our measurements of δC at a pressure of 11.31 bar are compared with a fit to Eq. (2) taking α to be temperature independent. The good agreement between the data and the calculated curve confirms that α is a constant with a best fit value of 0.48 ± 0.08 at this pressure. The significant down turn in δC near T_c in Fig. 2 is due to the strong temperature dependence of the coherence length. We have made this comparison at all pressures, and the results are presented together in Fig. 4. The scale factor appears to be both temperature *and* pressure independent with the average

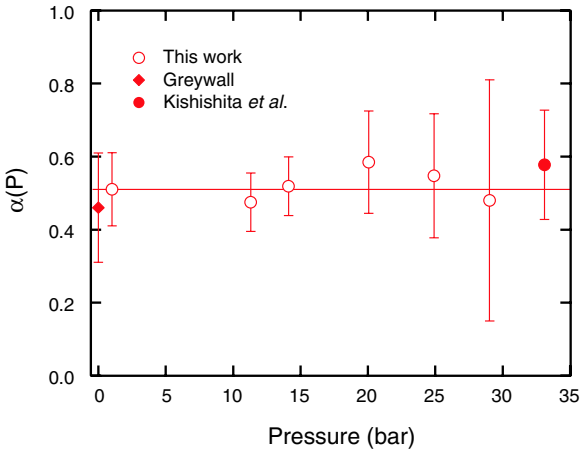

FIG. 4 (color online). The scale factor α for the surface heat capacity as a function of pressure. The present measurements are shown as open circles and are pressure independent with an average of $\alpha = 0.51$. There is good agreement with earlier work from Greywall [20] (diamond) and Kishishita *et al.* [22] (solid circle) interpreted in terms of our model.

value $\alpha = 0.51 \pm 0.15$. In the context of our model, this means that the spatial range for surface excitations, which we associate with quasiparticle bound states, is half of a coherence length.

Greywall [20] allowed for a healing length of superfluid ^{3}He near the silver heat exchanger surface in his measurement of specific heat, and he assumed its temperature dependence to have the form $(1 - (T/T_c)^4)^{-1/2}$. We have reanalyzed his data with our model as well as the work of Kishishita *et al.* [22]. Both results are plotted in Fig. 4, where they are compared directly to ours. It is noteworthy that the silver sinter used by Kishishita *et al.* had an area-to-volume ratio of 12×10^6 m^{-1}, the one in the Greywall experiment was 3.4×10^6 m^{-1}, and these can be compared with ours, 5.2×10^6 m^{-1}. There is excellent agreement among the experiments, although they are performed in a range of pore structures with area-to-volume ratios spanning a factor of 3. This implies that different structures among the silver sinters do not play a role. The overall consistency of the data with the model, including the variables of pressure, temperature, and different silver surface structures, provides compelling evidence that we are measuring a surface contribution to the heat capacity rather than the heat capacity of disconnected regions of superfluid with a distribution of transition temperatures. However, the model will not be correct close to the transition temperature where the coherence length diverges with increasing temperature approaching T_c. There is a point, nominally a few percent lower than T_c, where $\alpha\xi(T, P) = \alpha\xi_0(P)(1 - T/T_c)^{-1/2}$ reaches $V_1/A = 193$ nm. In our model, $\alpha\xi(T, P)A$ represents the volume of the surface bound states and, at this temperature, they would fill the silver exchanger of volume V_1. At 1.024 bar, this excluded temperature region is 3% of T_c; it decreases

with decreasing coherence length at higher pressure. Additionally, there is a small suppression of the transition temperature for ^{3}He in restricted geometry. These effects may account for difficulty in extending our model close to T_c and the corresponding systematic error from such an extrapolation in determining V_1 as is shown in Fig. 3.

From a theoretical perspective, quasiparticle scattering at the surface is responsible for a nonzero density of states at the Fermi level which should give a heat capacity that is linear in the temperature in the low temperature limit. Our model for the surface specific heat has this temperature dependence at low temperatures where $c_s = 0$ in Eq. (2). Additionally, the entropy at the transition temperature determined from the specific heat in the model is within a few percent of that of the normal fluid at T_c, as is required for a second order thermodynamic transition. Although Eq. (2) is highly phenomenological, it might be a useful guide over a wider range of temperature than we have explored. It gives a low temperature limit for the density of states, relative to the normal fluid, to be simply proportional to the pressure dependent coherence length $\alpha\xi_0(P)A/V_1$. It would be interesting to extend heat capacity experiments to lower temperatures for a direct measurement of the density of states of surface bound states.

In conclusion, we have used a high resolution method to determine the heat capacity of ^{3}He in the presence of a silver surface. We distinguish two different contributions: one from the bulk superfluid phase and the other from the ^{3}He near the silver surface. We have constructed a model based on low-energy contributions to the density of states associated with Andreev bound states of ^{3}He quasiparticles that scatter from the surface. We have found that the surface heat capacity has a temperature and pressure dependence given by the normal fluid specific heat and the bulk ^{3}He coherence length. Further, we determine that the spatial extent of the bound state region is one-half of the bulk ^{3}He coherence length. Our measurement of the heat capacity of ^{3}He in confined geometry provides independent evidence of surface bound states and supports recent results from surface sensitive measurements of the transverse acoustic impedance by Aoki *et al.* [15] and theoretical calculations of superfluid ^{3}He in slabs by Vorontsov and Sauls [7].

We acknowledge support from the National Science Foundation, DMR-0244099, and helpful discussions with Jim Sauls and Anton Vorontsov.

[1] A. A. Abrikosov and L. P. Gor'kov, Sov. Phys. JETP **12**, 1243 (1961); T. Tsuneto, Technical Report of the Institute of Solid State Physics, University of Tokyo, Series A, No. 47, 1962.
[2] A. F. Andreev, Zh. Eksp. Teor. Fiz. **46**, 1823 (1964) [Sov. Phys. JETP **19**, 1228 (1964)].
[3] M. Covington *et al.*, Phys. Rev. Lett. **79**, 277 (1997).
[4] Chia-Ren Hu, Phys. Rev. Lett. **72**, 1526 (1994).
[5] M. Fogelstrom, D. Rainer, and J. A. Sauls, Phys. Rev. Lett. **79**, 281 (1997).
[6] J. Kurkijarvi and D. Rainer, in *Helium Three*, Modern Problems in Condensed Matter Physics, edited by W. P. Halperin and L. Pitaevskii (North-Holland, Amsterdam, 1990), p. 313.
[7] A. B. Vorontsov and J. A. Sauls, Phys. Rev. B **68**, 064508 (2003).
[8] P. Sharma and J. A. Sauls, J. Low Temp. Phys. **125**, 115 (2001).
[9] W. P. Halperin and J. A. Sauls, cond-mat/0408593.
[10] H. Choi *et al.*, Phys. Rev. Lett. **93**, 145301 (2004).
[11] S. N. Fisher *et al.*, Phys. Rev. Lett. **91**, 105303 (2003).
[12] C. Bauerle *et al.*, Phys. Rev. B **57**, 14 381 (1998).
[13] A. M. Guenault and G. R. Pickett, in *Helium Three*, Modern Problems in Condensed Matter Physics, edited by W. P. Halperin and L. Pitaevskii (North-Holland, Amsterdam, 1990), p. 659.
[14] O. Avenel *et al.*, Phys. Rev. Lett. **47**, 803 (1981).
[15] Y. Aoki *et al.*, Phys. Rev. Lett. **95**, 075301 (2005).
[16] J. Xu and B. C. Crooker, Phys. Rev. Lett. **65**, 3005 (1990).
[17] A. Sachrajda *et al.*, Phys. Rev. Lett. **55**, 1602 (1985).
[18] J. C. Davis *et al.*, Phys. Rev. Lett. **60**, 302 (1988).
[19] M. R. Freeman *et al.*, Phys. Rev. Lett. **60**, 596 (1988); S. Miyawaki *et al.*, Phys. Rev. B **62**, 5855 (2000); K. Kawasaki *et al.*, Phys. Rev. Lett. **93**, 105301 (2004).
[20] D. S. Greywall, Phys. Rev. B **33**, 7520 (1986).
[21] R. Schrenk and R. Konig, Phys. Rev. B **57**, 8518 (1998).
[22] S. Kishishita, H. Kambara, and T. Mamiya, Phys. Rev. B **63**, 024512 (2001).
[23] D. Vollhardt and P. Wolfle, *The Superfluid Phases of* ^{3}He (Taylor & Francis, London, 1990).
[24] L. H. Kjaldman, J. Kurkijarvi, and D. Rainer, J. Low Temp. Phys. **33**, 577 (1978).